Egypt. J. Chem. **Vol. 66**, No. SI: 13 pp. 1633 - 1644 (2023)

Egyptian Journal of Chemistry

http://ejchem.journals.ekb.eg/

Thermal Treatment of Lead-Rich Dust to Improve Fresh Characteristics and Adsorption Behavior of Autoclaved Geopolymer for Methylene Blue Dye Removal

Ali M. Abdel-Aziz[a*], M. Ramadan[a], Alaa Mohsen[b], Mostafa A. Sayed[a]

[a] *Chemistry Department, Faculty of Science, Ain Shams University, Cairo 11566, Egypt*

[b] *Faculty of Engineering, Ain Shams University, Cairo 11566, Egypt*

Abstract

The main target behind this work is studying the synergistic returns of thermal treatment of Lead-rich sludge dust (LD) on fresh properties of alkali-activated geopolymer in addition to its adsorption performance towards the removal of methylene dye (MB) from aqueous media. According to TGA/DTGA analysis, the thermal treatment of received dust was at 500°C (TLD). Two geopolymeric pastes (Geo-LD and Geo-TLD) were prepared using NaOH solution. The binders of the first paste were composed of 50%slag +50%LD while the binders of the second paste were composed of 50%slag + 50%TLD; respectively. Regarding fresh properties, it was found that the initial/final-setting time (I/F-ST) of Geo-LD is longer than Geo-TLD by 472 and 535 min, respectively. Moreover, a significant increment in the spread area is observed from 38 cm^2 as in case of Geo-LD to 216 cm^2 for Geo-TLD. After alkali-hydrothermal activation, the measured compressive strength values at 5bars/4h for Geo-LD and Geo-TLD were 43 and 72 MPa; respectively. FTIR, X-ray diffraction (XRD), and Scanning electron microscopy (SEM) techniques confirmed that Geo-TLD activated powder contained zeolitic phases, calcium-silicate-hydrate (C-S-H), calcium-alumino-silicate-hydrate (C-A-S-H), and lead silicates. N_2-adsorption/desorption studies affirmed the high adsorption capacity of Geo-TLD activated powder. The generated product (Geo-TLD) was found to have a maximum MB adsorption capacity of 210 mg/g at the optimized conditions. The Langmuir isotherm model (R^2 = 0.9849) offers the best match and is the most appropriate for the experimental data. According to our results, MB adsorption on Geo-TLD takes place as monolayer adsorption on a surface with homogenous adsorption affinity. Moreover, the adsorption kinetics was better explained by the pseudo-second-order kinetic model.

Keywords: Geopolymer; Lead-rich sludge dust; Thermal treatment; Adsorption; Methylene blue; Compressive strength.

1. Introduction

Egypt has recently faced great challenges in reducing the negative effects of hazardous wastes, especially solid industrial wastes from many industries. Egypt occupies a great position in manufacturing many types of transparent and colored glass used for decorations, as well as glass crystals. The manufacture and polishing of glass crystals deplete special materials containing cerium, lead, and some polymers. Thus, the generated sludge/dust contains these hazardous ingredients. The proportion of lead in this waste reached 30%, cerium 4-7%, and organic content 6-10%, in addition to the existence of a high amount of reactive silica (40-60%) and calcium oxide (10-15%) [1, 2].

Many Egyptian researchers studied the recycling of this hazardous waste to produce environmentally friendly building materials [3, 4]. Abdel-Gawwad et al., 2019, 2020 and 2021 utilized lead-rich sludge dust (LD) to fabricate lightweight bricks as well as alkali-activated-geopolymers with reasonable mechanical properties in addition to anti-fungal and

*Corresponding author e-mail: alimostafa@sci.asu.edu.eg.; (Ali M. Abdel-Aziz).
EJCHEM use only: Received date 05 August 2023; revised date 14 August 2023; accepted date 21 August 2023
DOI: 10.21608/EJCHEM.2023.227260.8367

anti-bacterial activity [5-7]. Ramadan et al., 2021 confirmed that replacing slag with LD increased the silica and alumina content and reduced the calcium content. Therefore this structural change increased the addition of some unique properties to the resulting geopolymer, such as fire resistance at high temperatures that reached 1000^{o}C as well as resistance to high dosages of gamma rays that reached 3000 KGy [8]. Mohsen et al., 2022 developed eco-friendly and innovative cementitious blends based on LD; this study confirmed the pozzolanic activity of this waste and the high performance of fabricated building materials for radiation shielding applications. Ramadan et al., 2021 terminated that although pozzolanic cement containing LD was lower in compressive strength than pozzolanic cement containing soda glass, the latter has a lower performance towards blocking radiation [2]. Ramadan et al., 2023 developed a novel geopolymer based on 50% slag, 40% fly ash, and 10% LD. The alkali-hydrothermal activation of these binders stabilized lead and cerium to create lead silicate Pb_3SiO_5 and cerium silicate $Ce_2Si_2O_7$. Moreover, the porous structure of the prepared geopolymer was rearranged, under steam pressure, to increase BET surface area and total pore volume [9].

Despite the mentioned advantages of LD, it negatively affected the fresh properties of the pastes (setting times, workability, and rheology). This was attributed to the large organic content, which reached about 10%. Some researchers reported that LD has a high ability to absorb/adsorb water. To solve this problem, some researchers used high content of water (mixing water), which reached 40%, and others decided to use some superplasticizers [1, 8, 10, 11].

On the other hand, geopolymer possesses specific surface characteristics (crosslinking, negative charges, and porous structure); it has been used recently to treat wastewater that carries industrial dyes such as methylene blue dye [12-14]. Nowadays, various technologies have been applied to remove dyes from wastewater; among these technologies is the adsorption method because of the low cost and energy used and the possibility of application on a large scale [15-18]. Padmapriya et al., 2022 developed a low-cost adsorbent based on geopolymerizaion of slag, fly ash, and bottom ash for effective removal of methylene blue, while Alouani et al., 2018 used fly ash-based geopolymer [19, 20]. Metakaolin-based geopolymer was utilized by Jin et al., 2021 for rapidly removing nickel ions and methylene blue [21]. Al-husseiny et al., 2022 reported that 95% removal of methylene blue was achieved by magnetite/geopolymer composite [22].

The innovation in this work is studying the synergistic returns caused by the heat treatment of the received dust (LD) on the performance of slag-LD-based geopolymer: fresh properties (setting time and workability), compressive strength, as well as the adsorption behavior for removal of methylene blue from aqueous media.

2. Materials and Methodology

2.1. Materials

Waste materials (geopolymer binders) used in this work were amorphous slag, lead-rich sludge dust (LD), and thermally treated lead-rich dust (TLD) at 500^{o}C. Slag was received from Lafarge Egypt Company while the used dust was received from Asfour Crystal Company, Egypt. Chemical composition (XRF analysis) of waste materials is displayed in Table 1. The particle size distribution analyzer showed that 99% of the slag, LD and TLD particle sizes were 12.97, 8.86 and 10.77 μm, respectively. Methylene blue (MB) was purchased from Sigma–Aldrich.

2.2. Experimental routine

Thermogravimetric analyses (TGA/DTGA, NETZSCH) were conducted on the received dust up to 500^{o}C under N_2-atmosphere to explain what happens to LD when it is heated. The thermogram of LD in **Fig. 1** shows two successive mass losses %. The 1st mass loss up to 250^{o}C equals 4.7%, attributed to moisture and gradual dehydration of gypsum, while the 2nd loss (250-500°C) equals 12.1%, which is assigned to thermal removal of organic content [2, 23].

Two geopolymeric pastes (Geo-LD and Geo-TLD) were prepared using NaOH solution (6 mass% of total binders). The binders of the 1st paste were composed of 50%slag +50%LD while the binders of the 2nd paste were composed of 50%slag + 50%TLD, respectively. The dried binders of each geopolymer were prepared by mixing the tested binders for 1h in a ball mill; after that, the homogeneous binders were

activated by the prepared alkaline solution using an automatic mixer for 3 minutes to fabricate the fresh pastes. The water/binder ratio for Geo-LD and Geo-TLD was found to be 0.4 and 0.35, respectively.

The setting times of the fresh pastes were measured according to ASTM C191-19 using the Vicat apparatus [24]. The flowability of fresh pastes of Geo-LD and Geo-TLD was examined through a mini-slump. The fresh paste was poured into standard Abram's cone (1.90 ± 0.10 cm top diameter, 3.90 ± 0.10 cm bottom diameter and 5.90 ± 0.10 cm height) on a flat metal plate located on a vibrating table. The cone was vertically removed, then the paste flowed into a pancake form. Finally, the pancake's diameter was measured to calculate the spread area in cm^2 [25-29]. The fresh Geo-LD and Geo-TLD pastes were cast in a 1-inch cubic stainless-steel mold and then treated for 24h in high humidity (99%), then the hardened pastes were hydrothermally cured in an autoclave for 4h at 5bars. According to ASTM C109M-20b [30], the mean compressive strength values of 4 autoclaved cubes for Geo-LD and Geo-TLD were measured. After optimizing cementitious properties (setting times, flowability, and compressive strength), the selected geopolymer (Geo-TLD) was characterized using XRD, FTIR, and SEM.

After optimization, the toxicity characteristics leaching procedure (TCLP) was conducted to immobilize lead content [31]. 2.5 g from the crushed Geo-TLD was mingled with 100 ml acetic acid solution of pH =3 in an automatic orbital shaker at 200 rpm for 10h; then the solution was filtrated. A flame atomic absorption spectrometer (FAAS, model Perkin Elmer 3100) was used to measure the lead concentration in leachate (ppm).

2.3. Dye adsorption experiments

1000 ppm MB solution was prepared as a stock solution for further investigations, and it was progressively diluted as necessary. Adsorption tests in batch mode were performed by adding 0.03 g of Geo-TLD to a 100 mL stoppered glass holding 50 mL of a 20 ppm MB dye solution, and stirring it on a thermostatic orbital shaker at 250 rpm. Variables like pH (2–11), contact duration (0–180 min), the initial concentration of dye (10–300 ppm), and temperature (298–327.5 K) were studied in a series of batch adsorption studies. Samples were stirred at 250 rpm for 2h in order to ensure that adsorption equilibrium was attained in each batch adsorption test. Using a dual beam UV-vis spectrophotometer, the remaining dye concentrations were determined at 664 nm. Calibration curves were constructed prior to the measurement using the standard MB solutions with established concentrations. This formula can be used to calculate the dye clearance percentage:

$$\textbf{Removal percntage}(\%) = \frac{\mathbf{C_0 - C_t}}{\mathbf{C_0}} \times \mathbf{100} \quad (1)$$

where C_0 and C_t (mg/L) are the liquid-phase concentrations of dye at initial and any time (t), respectively. The equilibrium dye adsorption capacity, q_e (mg/g), was estimated using:

$$\mathbf{q_e} = \frac{\mathbf{(C_0 - C_e)V}}{\mathbf{W}} \quad (2)$$

Where $\mathbf{C_0}$ (mg/L) and $\mathbf{C_e}$ (mg/L) are dye concentrations at initial and equilibrium, respectively. The volume of the solution is V (L), and the mass of the dry sorbent utilized is W (g). The sorption capacity at any time, t, q_t (mg/g), was calculated by:

$$\mathbf{q_t} = \frac{\mathbf{(C_0 - C_t)V}}{\mathbf{W}} \quad (3)$$

where C_t (mg/L) is the liquid-phase concentration of dye at any time.

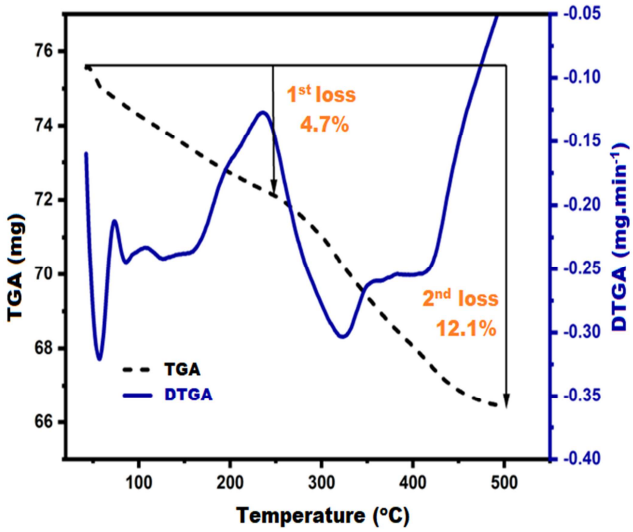

Fig.ure1: TGA/DTGA thermograms of received dust (LD)

3. Results and discussions

3.1 Cementitious properties

Fresh (setting time and workability) and hardened properties (compressive strength) are crucial parameters for assessing the suitability of developed geopolymeric composites in fabricating binding materials, therefore the setting time, workability, and

compressive strength were measured as displayed in **Table 2**.

Regarding the setting time, it is clarified that the initial/final-setting time (I/F-ST) of the Geo-LD is longer than Geo-TLD by 472 and 535 min, respectively. This indicates that the Geo-TLD is more applicable for producing binding materials than Geo-LD, as the I/F-ST of the Geo-TLD is in the acceptable range for binding materials, which falls between 45 and 375 min [32]. Generally, the presence of PbO_2 in Geo-LD and Geo-TLD composites causes retardation for the setting process. In the alkaline medium, the PbO_2 is transformed into $Pb(OH)_2$, which is formed on the composite's precursors, creating an isolating barrier between slag, LD/TLD and NaOH-solution and then poising the gepolymerization process [33]. The high organic content in the LD is the main reason for the long I/F-ST in the Geo-LD, as it acts as an impermeable membrane on the composite's constituent, delaying the geopolymerization reactions and hindering the formation of hydration products [8, 23]. Accordingly, the main reason behind the acceleration of I/F-ST of Geo-TLD concerning Geo-LD is the decomposition of organic resin after thermal treatment of LD at 500°C [2, 10].

For workability, a significant increment in the spread area is observed from 38 cm^2 for Geo-LD to 216 cm^2 for Geo-TLD (increment ≈ 468.4%). The poor workability of Geo-LD may be attributed to the high organic content that has a high capability to adsorb a high amount of water, which is required to improve workability [2]. Also, the presence of fine particles of LD (8.86 μm) compared to slag (12.97 μm) leads to (i) adsorption of free water [10]; (ii) increasing the interlocking between the matrix grains, entrapping huge quantities of free water [34]; and (iii) transforming the matrix mobile phase into stationary phase, resulting in increasing the viscosity [2]. Subsequently, the enhancement in the spread area values for Geo-TLD may result from removing organic matter and larger particle size TLD (10.77 μm) than LD (8.86 μm) after the thermal treatment process. Therefore, utilizing TLD in geoploymeric composites results in obtaining a workable/homogenous paste with a small quantity of water. This aligns with water/binder ratio values; it was decreased by 12.5% after utilizing TLD instead of LD, as a result, an improvement in mechanical properties is expected.

Concerning the mechanical properties, hydrothermal curing of the two geopolymeric composites at 5bars/4h causes obtaining a compressive strength close to (in the case of Geo-LD) and higher than (in the case of Geo-TLD) the Portland cement of grade 42.5-52.5 N/mm^2, referring to the ability to use the developed composited instead of cement. The progression in compressive strength with hydrothermal curing is owing to (i) motivating the geopolymerization reactions of aluminosilicate precursors (dissolution/condensation/polymerization) that result in the formation of strength-giving phases such as calcium-alumino-silicate-hydrate (C-A-S-H), calcium-silicate-hydrate (C-S-H), calcium-aluminum-hydrate (C-A-H) and sodium-alumino-silicate-hydrate (N-A-S-H) [35-39]. These products fill the pores as well as obtaining high gel/space-ratio and then enhancing mechanical properties [40-44]; (ii) developing the microstructure of the composites by creating a complex matrix from zeolitic phases as will be demonstrated by SEM [35]; and (iii) forming of Pb_3SiO_5 that acts as nucleation seeds for formation of more zeolitic phases as will be exhibited by XRD [11]. It is interesting to notice that the compressive strength of Geo-TLD is higher than Geo-LD by 67.4%. The significant enhancement after incorporating TLD in the matrix instead of LD may be due to the decomposition of organic matter that hinders the geopolymerization process and adsorps high water. Therefore, after organic matter removal, the geopolymerization process is enhanced and the water/binder ratio is decreased, forming a more compact microstructure [7]. According to XRF analysis, the chemical composition of LD is enhanced after thermal treatment by increasing Al_2O_3, SiO_2, and CaO wt.% by 50, 11.9 and 39.4%, respectively, than the received one, promoting the formation of further hydration binding phases [2]. Also, more hydration products are formed due to the high pozzolanic activity of TLD compared to LD [7]. Finally, it can be concluded that the cementitious properties of Geo-TLD are superior to Geo-LD, which makes Geo-TLD preferred to be employed as a binding material. Therefore, the Geo-TLD composite was selected to evaluate its efficiency in other applications as adsorbent material for hazardous dyes.

Table 1

Chemical oxide compositions (mass %) for geopolymer binders.

Waste materials	SiO_2	Al_2O_3	Fe_2O_3	CaO	PbO_2	MgO	SO_3	Na_2O	K_2O	Cl^-	LOI
Slag	51.62	12.71	0.30	25.41	0.00	7.30	1.83	0.48	0.18	0.04	0.10
LD	39.50	3.20	3.71	9.11	22.71	1.45	1.73	1.20	3.5	0.22	13.6
TLD	44.20	4.80	4.21	12.70	24.84	2.11	0.11	1.31	3.8	0.19	1.73

Table 2

Setting time, workability and compressive strength values of fabricated composites.

Tested properties	Geopolymeric paste	
	Geo-LD	Geo-TLD
Initial setting time/min	705	233
Final setting time/min	880	345
Spread area/cm^2	38	216
Compressive strength/MPa	43	72

3.2. Characterization of Geo-TLD powder

As the functional groups in the adsorbent materials greatly impact the mechanism explanation of the adsorption process, FTIR of the Geo-TLD was performed as in **Fig. 2a**. It is observed that the existence of six transmittance bands located at 410-518, 629-795, 840-1268, 1373-1572, 1610-1690 and 2550-3768 cm^{-1}, which are attributed to Si-O-Si/Pb-O-Si bending, Si-O-Al symmetric stretching, Si-O-Si (Al) asymmetric stretching, CO_3^{2-} symmetric stretching, H-O-H bending and O-H symmetric stretching, respectively. The 1st, 2nd and 3rd bands refer to the formation of geopolymeric chains and then successive geopolymerization process. The 1st band also indicates the immobilization of PbO_2 in the matrix through binding with silicate precursors and the creation of Pb-O-Si. This confirms the results obtained by XRD analysis that proved the transformation of PbO2 into Pb_3SiO_5 [8].

XRD-pattern **(Fig. 2b)** shows the synergistic impact of the alkali-activation and hydrothermal curing (5bars/4h) on the phase composition of the hydration products for Geo-TLD. It is noticed the appearance of highly-crystalline binding products such as hydrogarnet phase at 2θ= 28.1° (C-A-S-H, PDF# 00-020-0452) and tobermorite phase at 2θ= 29.4° (C-S-H, PDF# 00-033-0306). Also, a zeolitic phase from analcime is observed at 2θ= 26.3° ($NaAlSi_2O_6 \cdot H_2O$, PDF# 00-002-0417) due to the transformation of amorphous N-A-S-H to crystalline/cross-linked phase under high steam-pressure. These formed phases reinforce the microstructure of the developed composite (Geo-TLD), resulting in superior mechanical properties. Furthermore, crystalline peaks are identified at 2θ= 32.4, 47.3 and 56.1° referring to lead oxide (PbO_2, PDF# 00-037-0517), which results from incorporating TLD in the matrix. After hydrothermal curing, apart from the PbO_2 phase is stabilized by converting into lead silicate (Pb_3SiO_5, PDF# 00-032-0537), which appeared at 2θ=26.3, 28.1 and 29.4°. As illustrated above, the Pb_3SiO_5 supports the microstructure by acting as an active site for accumulating further hydration products [11, 45-48].

In general, the mechanical performance of the fabricated composite is significantly influenced by the microstructure of the matrix and the morphology of the generated hydrates. SEM-micrograph of the Geo-TLD **(Fig. 2c)** reveals pores-filling by crystalline zeolitic products from the analcime phase with a flower structure. This indicates the role of thermal treatment of LD and hydrothermal curing in forming a compact structure of strength-giving phases with high hydraulic nature [11].

As the fabricated geopolymeric composite Geo-TLD contains a high percentage of PbO_2 (12.42 wt.%), which has a hazardous impact on the environment and human health, the TCLP test was conducted to ensure the safety of utilizing this composite. **Table 3** clarifies the Pb-concentration (ppm) in the leachate solution. It is observed that the Pb-concentration of un-activated cementitious composite (50%slag+50%TLD without adding NaOH-solution) is very high (64.21 ppm). Interestingly, this concentration is significantly reduced to 0.43 ppm (lower than the toxicity limit) after activation and hydrothermal curing of the composite at 5bars/4h, indicating immobilization/stabilization of the Pb in the geopolymeric matrix, which proves the safety usage for the developed composite. The immobilization/stabilization mechanism can be discussed from several points of view, such as (i) the free-PbO_2 is transformed in the insoluble-Pb_3SiO_5) as confirmed by XRD and FTIR; (ii) the hydrothermal curing leads to alternating the texture characteristics by narrowing the pore as well as changing the geopolymeric chains into a cross-linked network that traps and encapsulates Pb; and (iii) the negative charge created on the Al center during the geopolymerization process supports the immobilization of Pb^{2+} ions [9].

Table3
Pb-concentrations (ppm) of the Geo-TLD composite in the leachate solution.

Specimen notation	Condition	Pb-concentration (ppm)
Geo-TLD	Un-activated	64.21
	Hydrothermally activated	0.43
Toxicity limit		≤5

3.3. Adsorption studies of MB onto Geo-TLD

3.3.1. Effect of pH on the adsorption capacity

The efficiency of geopolymers and other adsorbents is thought to be significantly influenced by their pH. Therefore, in the pH range of 2 to 11, the impact of the solution pH on MB uptake by Geo-TLD was investigated. The outcomes are shown in **Fig. 3a**. The removal effectiveness decreased from 91.0% to 74.5% when the pH rose from 3 to 7 but showed some signs of stability up to pH 11. The Geo-TLD showed a maximum dye removal at pH=3, this exceptional MB adsorption efficiency was further explained through offering Geo-TLD an acidic treatment at the ideal adsorption pH and monitoring the development with a surface area/pore size distribution analyzer (BET/BJH models).

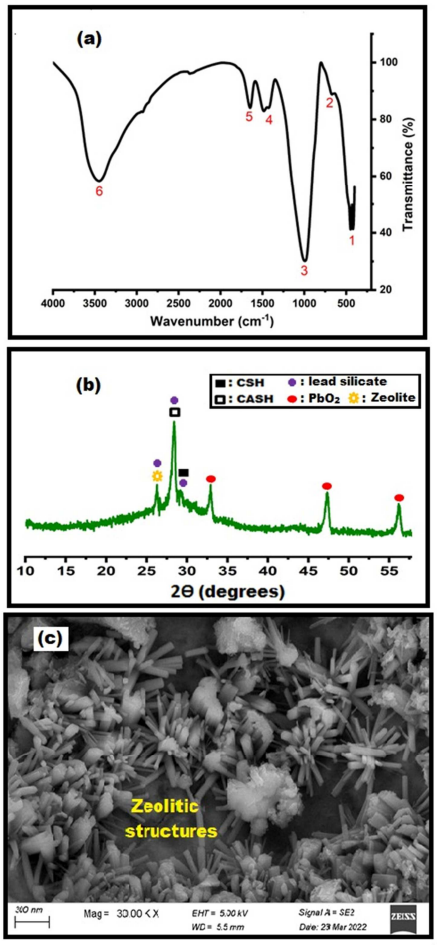

Figure 2: Geo-TLD powder characterization: (a) FTIR, (b) XRD and (c) SEM

To analyze the impact of the acidic treatment process at pH= 3 on the texture characteristics of the Geo-TLD, the N_2-adsorption/desorption isotherms were performed as illustrated in **Fig. 4 (a, b)**. It is observed that Geo-TLD before acidic treatment obeys type-III isotherm with H3-hysteresis, while after treatment, it obeys type-IV isotherm with H3-hysteresis **(Fig. 4)**. Generally, the isotherm type reflects the pores' type/shape which affected the adsorption behavior of the adsorbent materials. After the treatment process, it is found that BET-specific surface area, total pore volume, BJH-average pore

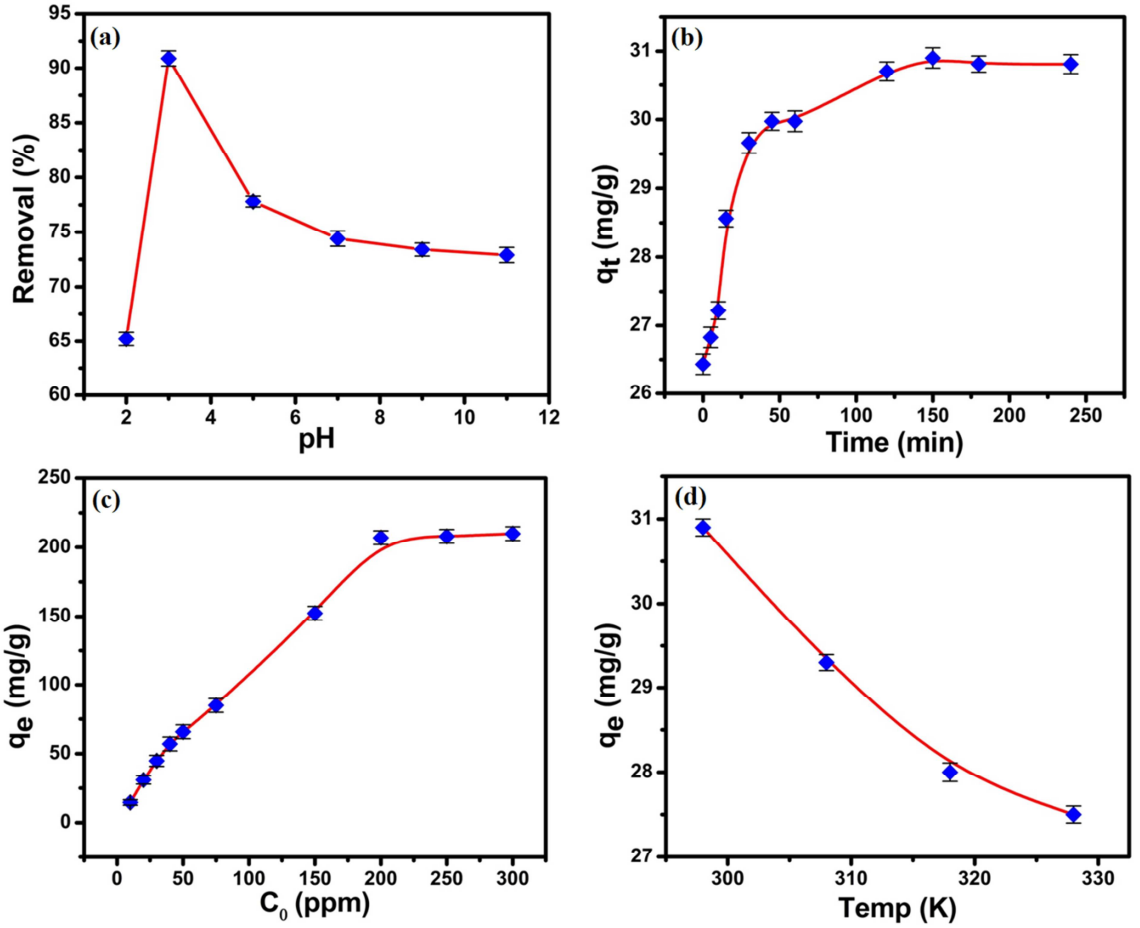

Figure 3: Effect of solution pH (a), contact time (b), initial concentrations (c), and temperature (d) on the adsorption of MB (C_o= 20 mg/L) onto Geo-TLD

Table 4

The main textural parameters of Geo-TLD before and after acidic treatment

Composite	BET-S.A (m^2/g)	Vt (cm^3/g)	Vm (cm^3/g)	dpmax (nm)	Isotherm type
Geo-TLD	23.66	0.150	5.43	18.80	III/H3
Acidified Geo-TLD	55.62	0.174	12.78	12.10	IV/H3

diameter and dpmax changed from 23.66 to 55.62 m^2/g, 0.150 to 0.174 cm^3/g, 5.43 to 12.78 cm^3/g and 18.80 to 12.10 nm, respectively. These findings confirmed the significant impact of acidic treatment process on improving the Geo-TLD composite adsorption capacity (**Table 4**). Also, the adsorption capacity in the acidic medium increases as the geopolymerization process event produces a negatively charged solid surface [49]; therefore, the strong alkaline medium creates a competition between a negatively charged geopolymer surface and OH^- ions on the adsorption of MB dye which decrease the adsorption efficiency [50, 51].

3.3.2. Effect of residence time on adsorption of MB

It was investigated how the contact time affected the MB adsorption on the Geo-TLD adsorbent. The adsorption capacity increased with increasing contact duration, as depicted in **Fig. 3b**.

The results demonstrated that the adsorption process is quite quick and that most of the dye is absorbed in the first 30 minutes, whilst the adsorbent achieved equilibrium in 120 minutes. The existence of free adsorption sites at the beginning of the dye adsorption process can be attributed to this quick adsorption. After the available sites were saturated and equilibrium was attained, there was no further adsorption **[52]**. This is in accordance with what several scholars have stated in the relevant literature **[53-55]**.

3.3.3. Effect of Initial Concentration on Adsorption of MB

The immediate interaction of the initial dye concentration with the adsorbent binding sites determines what happens next **[56]**. In the range of 10-300 mg L^{-1}, the impact of the initial amount of MB on the Geo-TLD adsorbent's overall performance at equilibrium was assessed. The amount of adsorbed MB in the solid phase at equilibrium rose linearly and considerably with rising MB concentrations, as shown in **Fig. 3c**. For instance, when the starting concentration was increased from 10 to 200 mg L^{-1}, the amount of MB adsorbed rose from 15 to 207 mg g^{-1}, reaching a maximum adsorption capacity of 210 mg g^{-1} at MB concentrations of 300 mg L^{-1} for the Geo-TLD sorbent. The loading capacity of the adsorbent grows along with the initial dye concentration until no more active sites are left to store further dye molecules **[57]**. A similar experiment discovered a pattern in such a factor's influence on MB adsorption **[58]**.

3.3.4. Effect of Temperature

The impact of temperature on Geo-TLD's adsorption capacity was taken into consideration, as illustrated in **Fig. 3d**. In this investigation, as the temperature was increased from 25 °C to 55 °C, the MB removal capacity declined from 31 mg g^{-1} to 27.5 mg g^{-1}. Enthalpy of adsorption and an exothermic reaction were attributed for the reported decline **[59, 60]**.

3.4. Adsorption Isotherms

The adsorption isotherm is important to figure out how Geo-TLD and MB interact with each other. The Langmuir **(Eq. (S1))**, Freundlich **(Eq. (S2))**, and Temkin **(Eq. (S3))** isotherm models were applied to model the equilibrium data obtained for MB on Geo-TLD. The Langmuir constants, q_m (the maximum adsorption capacity) and K_L, were estimated from the linear plot of C_e/q_e versus C_e **(Fig. 5a)** to be 231.5 (mg/g) and 0.054 (L/mg), respectively **(Table 5)**. The value of correlation coefficient (R^2 = 0.9849) obtained demonstrates that Langmuir expression offered a superior fit to the experimental data of MB on Geo-TLD. The equilibrium data were further analyzed using the Freundlich isotherm model by plotting log q_e versus log C_e **(Fig. S1A)** and the results summarized in **Table 5**. The correlation coefficient, R^2, was 0.9764 indicating good linearity. The results revealed that the value of n is more than unity (n = 2.4) confirming that the adsorption process of MB is favorable on Geo-TLD. The resulting equilibrium data was examined as well using the linear form of Temkin isotherm model **(Eq. (S3))**. **Table 5** lists the Temkin model variables, and the coefficient of correlation calculated from the slope and intercept of the linear plot of q_e versus lnC_e as displayed in **Figure S1B**. The correlation coefficient, R^2,

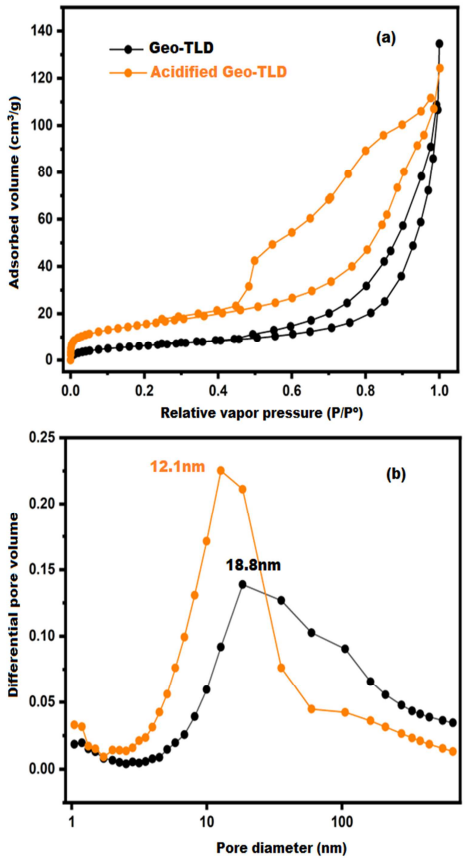

Figure4: (a) N_2 adsorption/desorption isotherms and (b) PSD curves for Geo-TLD before and after acidic treatment at pH = 3

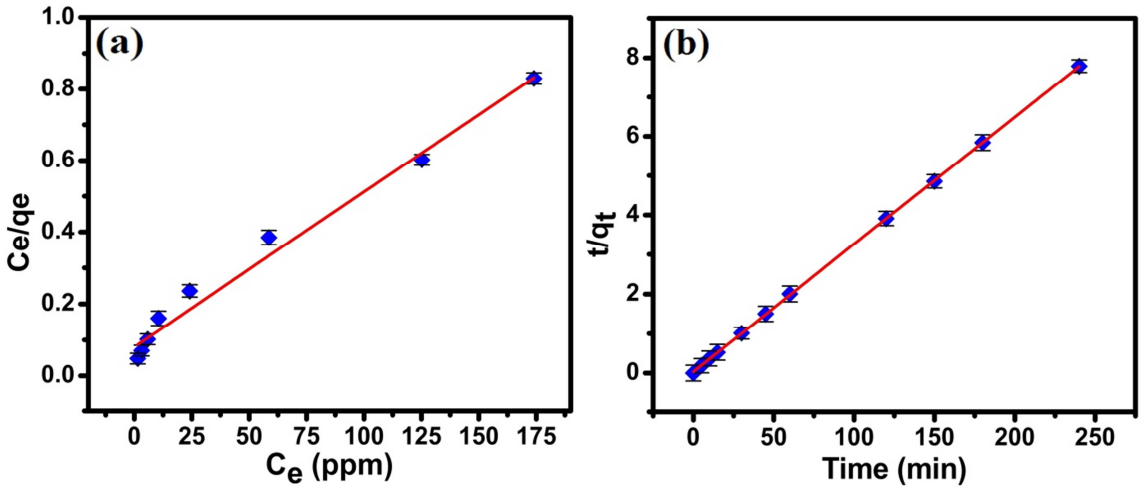

Figure 5: Liner plots of (a) Langmuir adsorption isotherm and (b) Pseudo-second-order kinetic model for adsorption of MB on Geo-TLD

Based on the reported values of the correlation coefficients for Langmuir, Freundlich, and Temkin isotherms, we can deduce that the Langmuir isotherm model is the most well-fitted and more appropriate to the experimental data than all other isotherms (R^2 = 0.9849). These findings show that MB adsorption on Geo-TLD occurs as monolayer adsorption on a surface with homogeneous adsorption affinity.

3.5. Kinetic Studies

The most prevalent kinetics models were utilized in order to assess the kinetics of adsorption and fit the experimental data. **Table 6** lists the coefficients of correlation as well as the kinetic parameters for the adsorption of MB onto Geo-TLD. The correlation coefficient, R^2, estimated from the linear plot of the pseudo-first-order kinetic model **(Eq. (S4)) (Fig. S2)** (R^2 = 0.9688) is lower than that determined from the linear plot of the pseudo-second-order kinetic model **(Eq. (S5)) (Figure 5b)** (R^2 = 0.9999). Furthermore, the value of q_e derived from the fitted linear plot of pseudo-second-order model (q_e = 30.98) matches with the experimental data ($q_{e,exp}$ = 31) better than that of the pseudo-first-order model (q_e = 4.01). According to **Table 6**, the pseudo-second-order kinetic model offered a better correlation for MB adsorption onto Geo-TLD than the pseudo-first-order model, and it was more acceptable to use the pseudo-second-order kinetic model to explain the adsorption kinetics.

Table 5
Parameters of the Langmuir, Freundlich and Temkin isotherms for the adsorption of MB on Geo-TLD

Isotherm	Parameters	Value
Langmuir	q_m (mg g^{-1})	231.5
	K_L (L mg^{-1})	0.054
	R^2	0.9849
Freundlich	K_F	25.95
	n	2.4
	R^2	0.9764
Temkin	K_T (L g^{-1})	1.04
	b_T (KJ mol^{-1})	40.76
	R^2	0.9169

Table 6
Kinetic parameters and their correlation coefficients for the adsorption of MB onto Geo-TLD

Model	Parameters	Value
Pseudo-first-order	K_1 (min^{-1})	0.024
	q_e (mg g^{-1})	4.01
	R^2	0.9688
Pseudo-second-order	K_2 (g mg^{-1} min^{-1})	0.03
	q_e (mg g^{-1})	30.98
	R^2	0.9999

4. Conclusion

Two different green geopolymeric composite pastes have been prepared via NaOH-activation; these pastes based on slag, lead-rich sludge dust (LD), and thermally treated dust at 500 °C (TLD). The cementitious characteristics such as setting times, workability, and compressive strength were

measured. The optimized geopolymeric powder was utilized as an efficient adsorbent for removal of methylene blue dye from aqueous media. The following points have been concluded:

- The received dust (LD) retarded geopolymerization process of Geo-LD (50% slag + 50% LD) due to high content of lead and organic resin.
- Compared with LD, TLD shortened setting times and enhanced flowability of the fresh paste.
- The hydrothermal activation of Geo-TLD (50% slag + 50% TLD) at 5bar/4h developed the compressive strength of the hardened paste up to 72MPa.
- The alkali/hydrothermal activation of Geo-TLD created some active centers and modified the textural characteristics which affirmed via FTIR, XRD, SEM, and BET/BJH techniques.
- TCLP test affirmed the safety of Geo-TLD as green building material, and it's recommended to use as mechanical resistance fillers for wastewater treatment.
- The impact of various factors like the pH, contact time, starting concentration, and temperature on the adsorption effectiveness of the Geo-TLD toward MB dye were studied and optimized.
- The Langmuir isotherm model (R^2 = 0.9849) offers the best match and is the most appropriate for the experimental data, as well as the maximum adsorption capacity of the optimized Geo-TLD was found to be 210 mg/g.
- According to our results, the adsorption kinetics was better explained by the pseudo-second-order kinetic model.

5. Conflicts of interest

The authors declared no potential conflicts of interest concerning this article's research, authorship, and/or publication.

6. References

[1] Y. Essam, N. El-Faramawy, W. Ramadan, M. Ramadan, From dangerous wastes to green construction materials, as thermally stable-radiation blocker, in presence of meso-porous magnesia and alumina, Journal of Building Engineering, (2023) 105896.

[2] A. Mohsen, M.S. Amin, S.A. Waly, M. Ramadan, Rheological behavior, mechanical properties, fire resistance, and gamma ray attenuation capability for eco-friendly cementitious mixes incorporating thermally treated lead sludge, Construction and Building Materials, 359 (2022) 129479.

[3] M.S. El-Feky, A. Mohsen, A. Maher El-Tair, M. Kohail, Microstructural investigation for micro - nano-silica engineered magnesium oxychloride cement, Construction and Building Materials, 342 (2022) 127976.

[4] A. Maher, M. Elfeky, A. Mohsen, M. Kohail, Properties of Nano Engineered Concrete Subjected to Accelerated Corrosion, Nanotechnologies in Construction A Scientific Internet-Journal, 13 (2021) 293-305.

[5] H.A. Abdel-Gawwad, S.A. Mohamed, M.S. Mohammed, Recycling of slag and lead-bearing sludge in the cleaner production of alkali activated cement with high performance and microbial resistivity, Journal of Cleaner Production, 220 (2019) 568-580.

[6] H.A. Abdel-Gawwad, A.M. Rashad, M.S. Mohammed, T.A. Tawfik, The potential application of cement kiln dust-red clay brick waste-silica fume composites as unfired building bricks with outstanding properties and high ability to CO_2-capture, Journal of Building Engineering, 42 (2021) 102479.

[7] H.A. Abdel-Gawwad, S.A. Sanad, M.S. Mohammed, A clean approach through sustainable utilization of cement kiln dust, hazardous lead-bearing, and sewage sludges in the production of lightweight bricks, Journal of Cleaner Production, 273 (2020) 123129.

[8] F. Shwita, N. El-Faramawy, W. Ramadan, M. Ramadan, Investigation of the mechanical properties, morphology and the attenuation behavior of gamma rays for OPC pastes mingled with two different glass wastes, Construction and Building Materials, 313 (2021) 125475.

[9] M. Ramadan, A.O. Habib, M.M. Hazem, M.S. Amin, A. Mohsen, Synergetic effects of hydrothermal treatment on the behavior of toxic sludge-modified geopolymer: Immobilization of cerium and lead, textural characteristics, and mechanical efficiency, Construction and Building Materials, 367 (2023) 130249.

[10] M. Ramadan, A.O. Habib, M. Kohail, A. Mohsen, Enhancement of fresh and hardened properties of geopolymeric composite containing toxic lead sludge: A comparative study between the effect of superplasticizer and thermal treatment of sludge, Journal of Building Engineering, 71 (2023) 106482.

[11] M. Ramadan, M. Kohail, Y.R. Alharbi, A.A. Abadel, A.S. Binyahya, A. Mohsen, Investigation of autoclave curing impact on the mechanical properties, heavy metal stabilization and anti-microbial activity of the green geopolymeric composite based on received/thermally-treated glass polishing sludge, Journal of Materials Research and Technology, 23 (2023) 2672-2689.

[12] R.M. Novais, J. Carvalheiras, D.M. Tobaldi, M.P. Seabra, R.C. Pullar, J.A. Labrincha, Synthesis of porous biomass fly ash-based

geopolymer spheres for efficient removal of methylene blue from wastewaters, Journal of cleaner production, 207 (2019) 350-362.
[13] Ö. Açışlı, İ. Acar, A. Khataee, Preparation of a surface modified fly ash-based geopolymer for removal of an anionic dye: Parameters and adsorption mechanism, Chemosphere, 295 (2022) 133870.
[14] A.A. Siyal, M.R. Shamsuddin, M.I. Khan, N.E. Rabat, M. Zulfiqar, Z. Man, J. Siame, K.A. Azizli, A review on geopolymers as emerging materials for the adsorption of heavy metals and dyes, Journal of Environmental Management, 224 (2018) 327-339.
[15] P. Rożek, M. Król, W. Mozgawa, Lightweight geopolymer-expanded glass composites for removal of methylene blue from aqueous solutions, Ceramics International, 46 (2020) 19785-19791.
[16] X. Feng, S. Yan, S. Jiang, K. Huang, X. Ren, X. Du, P. Xing, Green synthesis of the metakaolin/slag based geopolymer for the effective removal of methylene blue and Pb (II), Silicon, (2021) 1-15.
[17] A. Maleki, M. Mohammad, Z. Emdadi, N. Asim, M. Azizi, J. Safaei, Adsorbent materials based on a geopolymer paste for dye removal from aqueous solutions, Arabian Journal of Chemistry, 13 (2020) 3017-3025.
[18] M.A. Sayed, M. Ahmed, M. El-Shahat, I.M. El-Sewify, Mesoporous polyaniline/SnO_2 nanospheres for enhanced photocatalytic degradation of bio-staining fluorescent dye from an aqueous environment, Inorganic Chemistry Communications, 139 (2022) 109326.
[19] M. Padmapriya, S. Ramesh, V. Biju, Synthesis of seawater based geopolymer: Characterization and adsorption capacity of methylene blue from wastewater, Materials Today: Proceedings, 51 (2022) 1770-1776.
[20] M. Alouani, S. Alehyen, M. Achouri, M. Taibi, Removal of cationic dye-methylene blue-from aqueous solution by adsorption on fly ash-based geopolymer, Journal of Materials and Environmental Science, 9 (2018) 32-46.
[21] H. Jin, Y. Zhang, Q. Wang, Q. Chang, C. Li, Rapid removal of methylene blue and nickel ions and adsorption/desorption mechanism based on geopolymer adsorbent, Colloid and Interface Science Communications, 45 (2021) 100551.
[22] R.A. Al-husseiny, S.E. Ebrahim, Effective removal of methylene blue from wastewater using magnetite/geopolymer composite: Synthesis, characterization and column adsorption study, Inorganic Chemistry Communications, 139 (2022) 109318.
[23] H.A. Abdel-Gawwad, M.S. Mohammed, S.E. Zakey, Preparation, performance, and stability of alkali-activated-concrete waste-lead- bearing sludge composites, Journal of Cleaner Production, 259 (2020) 120924.
[24] ASTMC191-19, Standard Test Methods for Time of Setting of Hydraulic Cement by Vicat Needle, Annual Book of ASTM International Standards, West Conshohocken, PA, (2019).
[25] S.A. Arafa, A.Z.M. Ali, A.S.M.A. Awal, L.Y. Loon, Optimum mix for fly ash geopolymer binder based on workability and compressive strength, IOP Conference Series: Earth and Environmental Science, 140 (2018) 012157.
[26] A.M. Humad, K. Habermehl-Cwirzen, A. Cwirzen, Effects of fineness and chemical composition of blast furnace slag on properties of alkali-activated binder, Materials, 12 (2019) 3447.
[27] A.O. Habib, I. Aiad, T.A. Youssef, A.M. Abd El-Aziz, Effect of some chemical admixtures on the physico-chemical and rheological properties of oil well cement pastes, Construction and Building Materials, 120 (2016) 80-88.
[28] A.O. Habib, I. Aiad, F.I. El-Hosiny, A. Mohsen, Studying the impact of admixtures chemical structure on the rheological properties of silica-fume blended cement pastes using various rheological models, Ain Shams Engineering Journal, 12 (2021) 1583-1594.
[29] Z. Tan, S.A. Bernal, J.L. Provis, Reproducible mini-slump test procedure for measuring the yield stress of cementitious pastes, Materials and Structures, 50 (2017) 235.
[30] ASTMC109M-20b, Standard test method for compressive strength of hydraulic cement mortars (using 2-in. or [50-mm] cube specimens, Annual Book of ASTM International Standards, West Conshohocken, PA, (2020).
[31] Method-1311/USEPA, Test Method for Evaluationg Solid Waste, Physical/Chemical Methods. SW-846, third ed. US EPA, Washington, DC, (2018).
[32] M. Refaie, A. Mohsen, A.R. Nasr El-Sayed, M. Kohail, The Effect of Structural Stability of Chemical Admixtures on the NaOH Alkali-Activated Slag Properties, Journal of Materials in Civil Engineering, 35 (2023) 04022367.
[33] M. Keppert, Retarding Action of Various Lead (II) Salts on Setting of Portland Cement, Key Engineering Materials, 760 (2018) 43-48.
[34] A. Mohsen, M. Ramadan, M. Gharieb, A. Yahya, A. Soltan, M.M. Hazem, Rheological behaviour, mechanical performance, and anti-fungal activity of OPC-granite waste composite modified with zinc oxide dust, Journal of Cleaner Production, 341 (2022) 130877.
[35] Y. Wei, J. Wang, J. Wang, L. Zhan, X. Ye, H. Tan, Hydrothermal processing, characterization and leaching toxicity of Cr-added "fly ash-metakaolin" based geopolymer, Construction and Building Materials, 251 (2020) 118931.
[36] O.A. Mayhoub, A. Mohsen, Y.R. Alharbi, A.A. Abadel, A.O. Habib, M. Kohail, Effect of curing regimes on chloride binding capacity of geopolymer, Ain Shams Engineering Journal, 12 (2021) 3659-3668.
[37] A. Mohsen, M.S. El-Feky, A.M. El-Tair, M. Kohail, Effect of delayed microwaving on the strength progress of Green alkali activated cement composites, Journal of Building Engineering, 43 (2021) 103135.
[38] M. Refaat, A. Mohsen, E.-S.A.R. Nasr, M. Kohail, Utilization of optimized microwave sintering to produce safe and sustainable one-part alkali-activated materials, Scientific Reports, 13 (2023) 4611.

[39] Z. Khaled, A. Mohsen, A. Soltan, M. Kohail, Optimization of kaolin into Metakaolin: Calcination Conditions, mix design and curing temperature to develop alkali activated binder, Ain Shams Engineering Journal, 14 (2023) 102142.
[40] A.A. El Gindy, E.A. Gomaa, H.I. Abdelkader, A. Mohsen, A.O. Habib, The effect of a sulfonated naphthalene-based polymer on redox reaction data, potassium ferrocyanide complexation, and the compressive strength of Portland cement paste, Journal of Molecular Liquids, 356 (2022) 119000.
[41] A. Mohsen, I. Aiad, F.I. El-Hossiny, A.O. Habib, Evaluating the Mechanical Properties of Admixed Blended Cement Pastes and Estimating its Kinetics of Hydration by Different Techniques, Egyptian Journal of Petroleum, 29 (2020) 171-186.
[42] A.O. Habib, I. Aiad, F.I. El-Hosiny, A.M. Abd El-Aziz, Development of the fire resistance and mechanical characteristics of silica fume-blended cement pastes using some chemical admixtures, Construction and Building Materials, 181 (2018) 163-174.
[43] S. Abo-El-Enein, S. Hanafi, F. El-Hosiny, E.-S.H. El-Mosallamy, M. Amin, Effect of some acrylate—poly (ethylene glycol) copolymers as superplasticizers on the mechanical and surface properties of portland cement pastes, Adsorption Science & Technology, 23 (2005) 245-254.
[44] F. Selim, F. Hashem, M. Amin, Mechanical, microstructural and acid resistance aspects of improved hardened Portland cement pastes incorporating marble dust and fine kaolinite sand, Construction and Building Materials, 251 (2020) 118992.
[45] A. Mohsen, M. Kohail, A.A. Abadel, Y.R. Alharbi, M.L. Nehdi, M. Ramadan, Correlation between porous structure analysis, mechanical efficiency and gamma-ray attenuation power for hydrothermally treated slag-glass waste-based geopolymer, Case Studies in Construction Materials, 17 (2022) e01505.
[46] D. Sayed, F. El-Hosiny, S. El-Gamal, M. Hazem, M. Ramadan, Synergetic impacts of mesoporous α-Fe_2O_3 nanoparticles on the performance of alkali-activated slag against fire, gamma rays, and some microorganisms, Journal of Building Engineering, 57 (2022) 104947.
[47] M. Ramadan, A. Habib, M. Hazem, M. Amin, A. Mohsen, Synergetic effects of hydrothermal treatment on the behavior of toxic sludge-modified geopolymer: Immobilization of cerium and lead, textural characteristics, and mechanical efficiency, Construction and Building Materials, 367 (2023) 130249.
[48] M. Ramadan, M. Kohail, A.A. Abadel, Y.R. Alharbi, R. Tuladhar, A. Mohsen, De-aluminated metakaolin-cement composite modified with commercial titania as a new green building material for gamma-ray shielding applications, Case Studies in Construction Materials, 17 (2022) e01344.
[49] P. Hadi, J. Guo, J. Barford, G. McKay, Multilayer Dye Adsorption in Activated Carbons—Facile Approach to Exploit Vacant Sites and Interlayer Charge Interaction, Environmental Science & Technology, 50 (2016) 5041-5049.
[50] G.Z. Kyzas, N.K. Lazaridis, A.C. Mitropoulos, Removal of dyes from aqueous solutions with untreated coffee residues as potential low-cost adsorbents: Equilibrium, reuse and thermodynamic approach, Chemical Engineering Journal, 189-190 (2012) 148-159.
[51] A.T. Mohd Din, B.H. Hameed, A.L. Ahmad, Batch adsorption of phenol onto physiochemical-activated coconut shell, Journal of Hazardous Materials, 161 (2009) 1522-1529.
[52] P. Hadi, J. Guo, J. Barford, G. McKay, Multilayer Dye Adsorption in Activated Carbons ・ Facile Approach to Exploit Vacant Sites and Interlayer Charge Interaction, Environmental Science & Technology, 50 (2016) 5041-5049.
[53] A.T.M. Din, B. Hameed, A.L. Ahmad, Batch adsorption of phenol onto physiochemical-activated coconut shell, Journal of Hazardous Materials, 161 (2009) 1522-1529.
[54] G.Z. Kyzas, N.K. Lazaridis, A.C. Mitropoulos, Removal of dyes from aqueous solutions with untreated coffee residues as potential low-cost adsorbents: Equilibrium, reuse and thermodynamic approach, Chemical engineering journal, 189 (2012) 148-159.
[55] S. El-Gamal, M. Amin, M. Ahmed, Removal of methyl orange and bromophenol blue dyes from aqueous solution using Sorel's cement nanoparticles, Journal of environmental chemical engineering, 3 (2015) 1702-1712.
[56] M.A.M. Salleh, D.K. Mahmoud, W.A.W.A. Karim, A. Idris, Cationic and anionic dye adsorption by agricultural solid wastes: a comprehensive review, Desalination, 280 (2011) 1-13.
[57] N. Kannan, M.M. Sundaram, Kinetics and mechanism of removal of methylene blue by adsorption on various carbons—a comparative study, Dyes and pigments, 51 (2001) 25-40.
[58] O.S. Amuda, A.O. Olayiwola, A.O. Alade, A.G. Farombi, S.A. Adebisi, Adsorption of methylene blue from aqueous solution using steam-activated carbon produced from Lantana camara stem, Journal of Environmental Protection, 5 (2014) 1352.
[59] L. Li, S. Wang, Z. Zhu, Geopolymeric adsorbents from fly ash for dye removal from aqueous solution, Journal of colloid and interface science, 300 (2006) 52-59.
[60] M.A. Al-Ghouti, M. Khan, M.S. Nasser, K. Al Saad, O. Ee Heng, Application of geopolymers synthesized from incinerated municipal solid waste ashes for the removal of cationic dye from water, Plos one, 15 (2020) e0239095.